



HAL
open science

On the causes of trends in the seasonal amplitude of atmospheric CO₂

Shilong Piao, Zhuo Liu, Yilong Wang, Philippe Ciais, Yitong Yao, Shushi Peng, Frédéric Chevallier, Pierre Friedlingstein, Ivan Janssens, Josep Penuelas, et al.

► **To cite this version:**

Shilong Piao, Zhuo Liu, Yilong Wang, Philippe Ciais, Yitong Yao, et al.. On the causes of trends in the seasonal amplitude of atmospheric CO₂. *Global Change Biology*, 2017, 24 (2), pp.608-616. 10.1111/gcb.13909 . hal-02900868

HAL Id: hal-02900868

<https://hal.science/hal-02900868>

Submitted on 14 Dec 2023

HAL is a multi-disciplinary open access archive for the deposit and dissemination of scientific research documents, whether they are published or not. The documents may come from teaching and research institutions in France or abroad, or from public or private research centers.

L'archive ouverte pluridisciplinaire **HAL**, est destinée au dépôt et à la diffusion de documents scientifiques de niveau recherche, publiés ou non, émanant des établissements d'enseignement et de recherche français ou étrangers, des laboratoires publics ou privés.

On the causes of trends in the seasonal amplitude of atmospheric CO₂

Shilong Piao^{1,2,3}  | Zhuo Liu¹ | Yilong Wang⁴ | Philippe Ciais⁴ | Yitong Yao¹ | Shushi Peng¹ | Frédéric Chevallier⁴ | Pierre Friedlingstein⁵ | Ivan A. Janssens⁶ | Josep Peñuelas^{7,8} | Stephen Sitch⁹ | Tao Wang^{2,3} 

¹Sino-French Institute for Earth System Science, College of Urban and Environmental Sciences, Peking University, Beijing, China

²Key Laboratory of Alpine Ecology and Biodiversity, Institute of Tibetan Plateau Research, Chinese Academy of Sciences, Beijing, China

³Center for Excellence in Tibetan Earth Science, Chinese Academy of Sciences, Beijing, China

⁴Laboratoire des Sciences du Climat et de l'Environnement, CEA CNRS UVSQ, Gif-sur-Yvette, France

⁵College of Engineering, Mathematics and Physical Sciences, University of Exeter, Exeter, UK

⁶Department of Biology, University of Antwerp, Wilrijk, Belgium

⁷CREAF, Barcelona, Catalonia, Spain

⁸CSIC, Global Ecology Unit CREAF- CSIC-UAB, Barcelona, Catalonia, Spain

⁹College of Life and Environmental Sciences, University of Exeter, Exeter, UK

Correspondence

Shilong Piao, Sino-French Institute for Earth System Science, College of Urban and Environmental Sciences, Peking University, Beijing, China.
Email: slpiao@pku.edu.cn

Funding information

National Natural Science Foundation of China, Grant/Award Number: 41530528; BELSPO STEREO project ECOPROPHET, Grant/Award Number: SR00334; 111 Project, Grant/Award Number: B14001; National Youth Top-notch Talent Support Program in China; European Research Council through Synergy grant, Grant/Award Number: ERC-2013-SyG-610028

Abstract

No consensus has yet been reached on the major factors driving the observed increase in the seasonal amplitude of atmospheric CO₂ in the northern latitudes. In this study, we used atmospheric CO₂ records from 26 northern hemisphere stations with a temporal coverage longer than 15 years, and an atmospheric transport model prescribed with net biome productivity (NBP) from an ensemble of nine terrestrial ecosystem models, to attribute change in the seasonal amplitude of atmospheric CO₂. We found significant ($p < .05$) increases in seasonal peak-to-trough CO₂ amplitude (AMP_{P-T}) at nine stations, and in trough-to-peak amplitude (AMP_{T-P}) at eight stations over the last three decades. Most of the stations that recorded increasing amplitudes are in Arctic and boreal regions (>50°N), consistent with previous observations that the amplitude increased faster at Barrow (Arctic) than at Mauna Loa (subtropics). The multi-model ensemble mean (MMEM) shows that the response of ecosystem carbon cycling to rising CO₂ concentration (eCO₂) and climate change are dominant drivers of the increase in AMP_{P-T} and AMP_{T-P} in the high latitudes. At the Barrow station, the observed increase of AMP_{P-T} and AMP_{T-P} over the last 33 years is explained by eCO₂ (39% and 42%) almost equally than by climate change (32% and 35%). The increased carbon losses during the months with a net carbon release in response to eCO₂ are associated with higher ecosystem respiration due to the increase in carbon storage caused by eCO₂ during carbon uptake period. Air-sea CO₂ fluxes (10% for AMP_{P-T} and 11% for AMP_{T-P}) and the impacts of land-use change (marginally significant 3% for AMP_{P-T} and 4% for AMP_{T-P}) also contributed to the CO₂ measured at Barrow, highlighting the role of these factors in regulating seasonal changes in the global carbon cycle.

KEYWORDS

amplitude of atmospheric CO₂, attribution, climate change, CO₂ fertilization effect, detection, land-use change

1 | INTRODUCTION

As an integrated signal of large-scale ecological changes, the change in seasonal variations of atmospheric CO₂ concentration is an emerging property of the carbon cycle (Bacastow, Keeling, & Whorf, 1985; Barlow, Palmer, Bruhwiler, & Tans, 2015; Forkel et al., 2016; Graven et al., 2013; Gray et al., 2014; Keeling, Chin, & Whorf, 1996; Kohlmaier et al., 1989; Piao et al., 2008; Randerson, Thompson, Conway, Fung, & Field, 1997; Wenzel, Cox, Eyring, & Friedlingstein, 2016; Zeng et al., 2014). The seasonal CO₂ amplitude (AMP) in the lower troposphere has increased by $\approx 50\%$ north of 45°N since the 1960s (Graven et al., 2013), and this signal has been suggested to be contributed by an increased seasonality of net biome productivity (NBP) in boreal and northern temperate ecosystems. A full understanding of the major factors governing the increase in NBP or the quantitative contribution of other, smaller fluxes such as fossil fuel CO₂ emissions and air-sea exchange to the increase in AMP is still lacking. On the one hand, Gray et al. (2014) and Zeng et al. (2014) suggested that agricultural improvements contributed to the increase in AMP at Mauna Loa by increasing the seasonal NBP uptake in cultivated lands, but the estimated contribution of this mechanism differed two-fold between the two studies (range 17%–45% of the increasing AMP). On the other hand, Randerson et al. (1997) and Forkel et al. (2016) showed that during the last three decades, most of the increase in amplitude took place at stations north of 55°N. In this view, agriculture improvement seems unlikely to be the only driving factor, because croplands are mainly in northern temperate latitudes (Foley et al., 2005). Using the LPJmL carbon cycle model with an improved phenological module coupled with an atmospheric transport model, Forkel et al. (2016) found that it is mainly the physiological response of northern plants to warming rather to increasing CO₂ that explains the trend of AMP over the last 20 years, but Graven et al. (2013) showed that AMP increased in the 1960s to the mid-1970s at a time when northern temperature slightly decreased. Moreover, Barnes, Parazoo, Orbe, and Denning (2016) suggested that advective fluxes through isentropic transport from mid-latitude surface fluxes play a larger impact than changes in Arctic fluxes on the northern high-latitude seasonal cycle throughout most of the troposphere, using GEOS-Chem chemical transport model with CO₂ fluxes simulated from CLM4.5. It therefore highlights the need to search deeper in the attribution of the AMP trend.

In this paper, we investigate the AMP trend in the Northern Hemisphere over the last thirty years (1980–2012) using an ensemble of ecosystem models with different parameterizations of the effects of elevated CO₂, climate change and land-use change (TRENDYv2; Sitch et al., 2015) with another transport model (LMDZ4; Hourdin et al., 2013). We also separate the contribution of fossil fuel CO₂ emissions, air-sea fluxes as well as the effects of climate change, rising CO₂ concentration (eCO₂), land-use change and nitrogen deposition in some models on the trends in the seasonality of land ecosystem carbon cycle. The contribution of atmospheric transport trends to AMP trends is also analyzed. We use long-term

(>15 years during 1980–2012) trends in seasonal atmospheric CO₂ concentrations from 26 northern (north of 23°N) atmospheric stations of the NOAA-ESRL surface flask air-sampling network (Table S1 and Fig. S1).

2 | MATERIALS AND METHODS

2.1 | Datasets

2.1.1 | Atmospheric CO₂ concentration data

Weekly data for atmospheric CO₂ concentration were obtained for 1980–2012 from the archive of Earth System Research Laboratory, National Oceanic and Atmospheric Administration (NOAA-ESRL; Masarie, Peters, Jacobson, & Tans, 2014). Our analyses used data from 26 northern temperate and boreal stations with observations longer than 15 years (Table S1), because the focus of our study was the long-term trend, which would not be robust without long-term observations. The seasonal curves of atmospheric CO₂ for each station were extracted by fitting the observation data with a function consisting of a quadratic polynomial for the long-term trend, four-harmonics for the annual cycle, and a 80-days Full-Width Half-Maximum value (FWHM) averaging filter and a 390-days FWHM averaging filter to further remove short term variations and remaining annual cycles still present in the residuals after the function fit (Thoning, Tans, & Komhyr, 1989). The processing was incorporated in the standard software for processing CO₂ data (CCGCRV) developed by NOAA-ESRL (Thoning et al., 1989). We then obtained the amplitude and monthly concentration differences from the seasonal curve for atmospheric CO₂.

2.1.2 | Land-atmosphere CO₂ exchange

An ensemble of eight dynamic global vegetation models (DGVMs) from TRENDYv2 was used to simulate monthly net biome productivity (NBP) for 1979–2012. These models were coordinated to perform three simulations (S1, S2, and S3) following the TRENDYv2 protocol (Sitch et al., 2015). Only atmospheric CO₂ was varied in simulation S1, and only atmospheric CO₂ and climate were varied in simulation S2. In simulation S3, atmospheric CO₂, climate and land use were varied. The effects of rising atmospheric CO₂, climate change and land use change on NBP could then be obtained from S1, the difference between S2 and S1, and the difference between S3 and S2, respectively. Four of the eight TRENDY models (CLM4.5, ISAM, LPX and OCN) considered carbon-nitrogen interactions and nitrogen deposition in simulation S1, S2, and S3. All models used the same forcing data sets, in which global atmospheric CO₂ concentration was from the combination of ice core records and atmospheric observations (Keeling & Whorf, 2005), historical climatic fields were from the CRU-NCEP dataset (<http://dods.extra.cea.fr/data/p529viov/cruncep/>), and land-use data were from the Hyde database (Hurtt et al., 2011). The effect of nitrogen deposition was derived from an additional simulation (S4) by the CLM4 model (Mao

et al., 2013; Oleson et al., 2010) in which all driving factors (atmospheric CO₂, climate and land use) were kept constant at the 1980 value, except transient nitrogen deposition for 1980–2012 (Lamarque et al., 2005). Strictly speaking, the effect of climate change on NBP contains the fingerprint of rising CO₂ since CO₂-induced climate change cannot be teased out based on offline simulations of carbon fluxes. The pure effect of climate change can only be obtained through resorting to the fully coupled earth system models (Mao et al., 2017), however which exist a lot of biases in terms of the simulated climate fields, CO₂ concentration and other biogeochemical processes. Detailed information of the nine DGVMs used in this study is listed in Table S2.

2.1.3 | Ocean-atmosphere CO₂ exchange

A biogeochemical model, PlankTOM5, combined with a global ocean general circulation model NEMO (NEMO-PlankTOM5), were used to simulate the physical, chemical and biological processes that affect the surface ocean CO₂ concentration and thus the ocean-atmosphere CO₂ exchange (Buitenhuis, Rivkin, Sailley, & Le Quéré, 2010). The PlankTOM5 model was forced by inputs of ions and compounds from river, sediment and dust (Aumont, Maier-Reimer, Blain, & Monfray, 2003; Cotrim da Cunha, Buitenhuis, Le Quéré, Giraud, & Ludwig, 2007). The NEMO model was driven by data for daily wind and precipitation from an NCEP reanalysis (Kalnay et al., 1996). Further details can be found in Buitenhuis et al. (2010).

2.1.4 | Fossil fuel CO₂ emissions

A gridded monthly time series of fossil fuel CO₂ emissions from CDIAC were constructed based on a proportional-proxy approach (Andres, Gregg, Losey, Marland, & Boden, 2011; Boden, Marland, & Andres, 2016). First, available monthly data for fossil fuel consumption data for 21 countries were compiled, which accounted for about 80% of global total emissions. These data were then used as a proxy for all remaining countries without monthly data based on countries' similarities in climates and economies (for few countries, geographic closeness was also considered). For some years without explicit monthly data, Monte Carlo methods were used to apply data from years with known monthly fractions to the years with missing-data. Further details can be found in Andres et al. (2011).

2.1.5 | The atmospheric transport model

We used LMDZ4, a global tracer transport model (Hourdin et al., 2013) driven by the re-analysis 3-D atmospheric wind fields from the European Centre for Medium-Range Weather Forecasts (Dee et al., 2011), to transform land-atmosphere CO₂ exchange, fossil fuel CO₂ emission and ocean-atmosphere CO₂ exchange into point estimates of CO₂ concentration for the 26 stations. The model configuration we used had a horizontal spatial resolution of 3.75° longitude × 2.5° latitude with 19 vertical layers.

The effects of changes in atmospheric CO₂ ("CO₂"), climate ("CLIM"), land use ("LU"), fossil fuel ("FF"), ocean carbon flux ("Ocean"), and atmospheric transport ("Wind") on seasonal change in atmospheric CO₂ concentration were differentiated by designing eight transport simulations (T1–T8, see Table S4). The first (T1) used time-varying monthly land-atmosphere CO₂ exchange under scenario S3 (driven by rising CO₂, climate change and land-use change), fossil fuel CO₂ emission, and ocean-atmosphere CO₂ exchange coupled with the LMDZ4 transport model with variable winds, indicating the combined effects of "CO₂", "CLIM", "LU", "FF", "Ocean", and "Wind". The LMDZ4 transport experiment was forced by historically varying wind but constant land-atmosphere CO₂ exchange, fossil fuel CO₂ emission, and ocean-atmosphere CO₂ exchange for 1979 (T6) to assess the contribution of "Wind". The individual effects of "CO₂", "CLIM", and "LU" were determined using the LMDZ4 model with varying winds to perform three more transport simulations (T2, T3 and T4, see Table S3), in which fossil fuel CO₂ emission and ocean-atmosphere CO₂ exchange were constant at the 1979 value but land-atmosphere CO₂ exchange varied under the three scenarios (S1, driven by CO₂; S2, driven by CO₂ and CLIM; S3, driven by CO₂, CLIM, and LU). Consequently, the effect of "CO₂" alone on seasonal CO₂ variation could be assessed by the difference between T2 and T6, that of "CLIM" by the difference between T3 and T2, and that of "LU" by the difference between T4 and T3. We also prescribed varying land-atmosphere CO₂ exchange from the CLM4 model under scenario S4 (varying only nitrogen deposition), constant fossil fuel CO₂ emission and ocean-atmosphere CO₂ exchange to the LMDZ4 model with constant winds (transport simulation T5) to obtain the effect of nitrogen deposition. Finally, we performed two more simulations in which only fossil fuel CO₂ emission or ocean-atmosphere CO₂ exchange varied in addition to variable winds (T7 and T8) to obtain the individual effects of "FF" and "Ocean" on CO₂ seasonal variation. The contribution of "FF" could thus be calculated from the difference between T7 and T6, and that of "Ocean" from the difference between T8 and T6.

3 | OBSERVED CO₂ AMPLITUDE TRENDS

The 26 northern (north of 23°N) atmospheric stations selected are shown in Fig. S1 and Table S1. According to the shape of detrended CO₂ seasonal cycle (Thoning et al., 1989; see Section 2; Fig. S2), we divided the amplitude into peak-to-trough (AMP_{p-t}, defined as the difference between the peak and trough values of the CO₂ seasonal cycle in a year) and trough-to-peak (AMP_{t-p}, defined as the difference between the trough value of the CO₂ seasonal cycle in a year and the peak value of the cycle in the next year). The AMP_{p-t} and AMP_{t-p} represent the seasonal variations in atmospheric CO₂ concentration during the period of net carbon uptake and the period of net carbon release, respectively (Fig. S2). Positive trends in AMP_{p-t} ranging from 0.05 to 0.15 ppm/year are significant ($p < .05$) at nine stations during 1980–2012, eight of which are north of 50°N

(Figure 1a). The other stations do not show significant positive AMP_{P-T} trends and five stations show negative trends (the latter being significant at only one station UUM). The significant increase in AMP_{P-T} mainly reflects an increasing CO₂ drawdown (defined by the monthly net change in CO₂ concentration) in June and July (Fig. S3).

The trends in AMP_{T-P} reported in Table S1 are similar to those of AMP_{P-T}, logically expected because we remove a long-term mean trend in each CO₂ time series (Figure 1b). In total, seven of the eight stations with a significant ($p < .05$) increase in AMP_{T-P} during 1980–2012 are located north of 50°N. The months of September and October are those during which most of the negative trend of AMP_{T-P} occurs at those stations (Fig. S3). Overall, no stations show significant positive trend in AMP_{T-P} during the study period.

4 | TERRESTRIAL ECOSYSTEM MODEL OUTPUT AND SIMULATION OF TRENDS IN CO₂ AMPLITUDE

The net biome productivity (NBP) from eight dynamic global vegetation models (DGVMs) from TRENDYv2 (Sitch et al., 2015) and an additional model with carbon-nitrogen interactions (Mao et al., 2013; Oleson et al., 2010; Tables S2 and S3) are prescribed to the atmospheric transport model (LMDZ4; Hourdin et al., 2013; see Section 2). Time-varying monthly NBP of each model from TRENDYv2 under simulation S3 (driven by CO₂, climate change and land-cover change; Sitch et al., 2015), fossil fuel and cement emissions (Andres et al., 2011; Boden et al., 2016), and interannual air-sea fluxes (Buitenhuis et al., 2010) were prescribed to the global LMDZ4

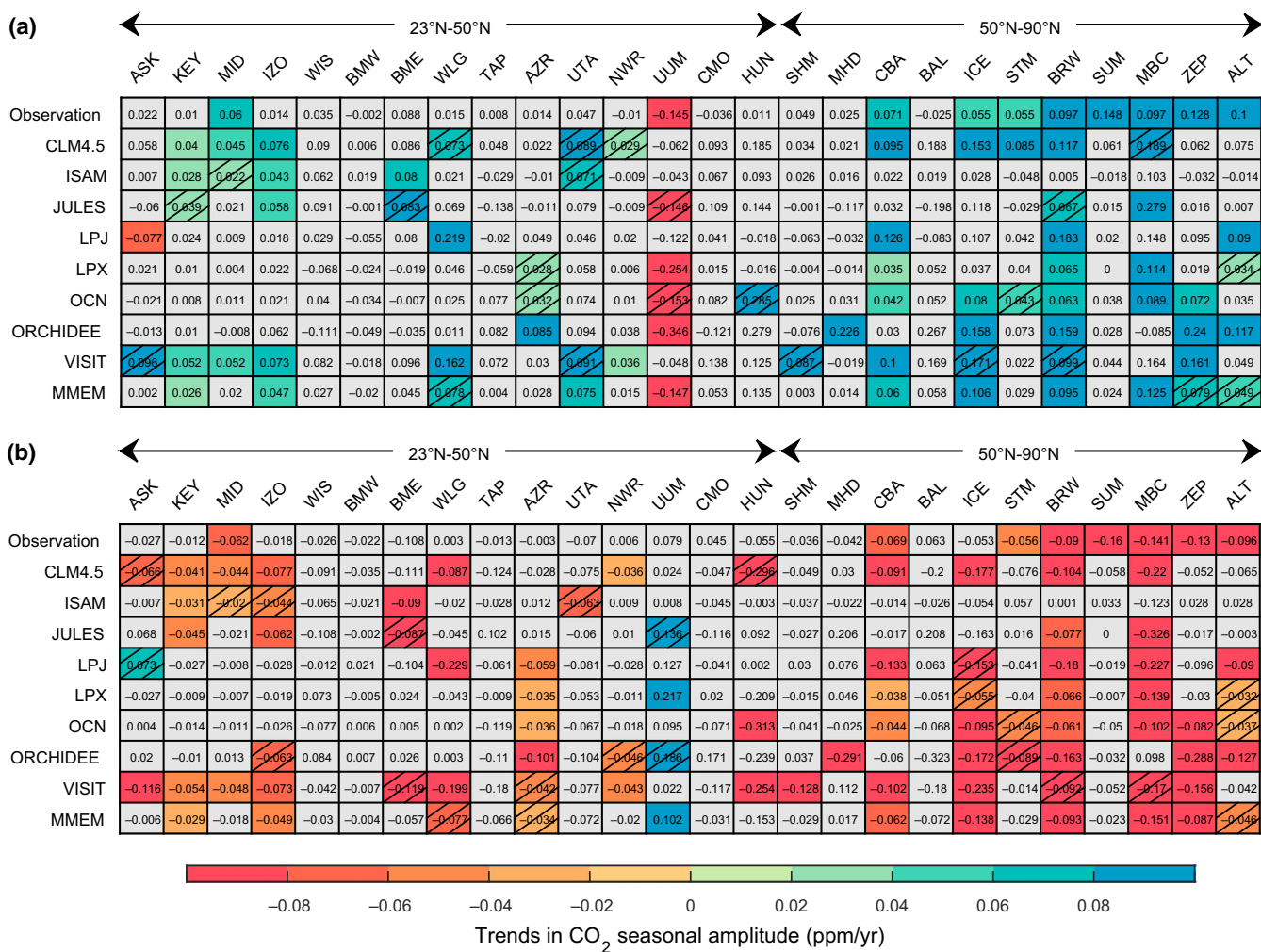


FIGURE 1 Observed and modeled trends in CO₂ seasonal peak-to-trough amplitude (AMP_{P-T}) (a) and trough-to-peak amplitude (AMP_{T-P}) (b) during 1980–2012. The modeled AMP_{P-T}/AMP_{T-P} trends were calculated based on eight TRENDY models and the multi-model ensemble mean (MMEM) in the T1 transport simulation (see Section 2). The abbreviated names of the 26 stations measuring atmospheric CO₂ concentrations in the northern temperate and boreal regions are shown at the top of the figure. The stations were sorted based on their latitudes, from 23 to 90°N. Each row represents the trends for the various stations, and each column represents the trends derived from observation and the model simulations at a station. Gray grids indicate non-significant trends ($p > .10$), colored grids without slashes indicate significant trends ($p < .05$) and colored grids with slashes indicate marginally significant trends ($p < .10$). The number in each grid is the value of the trend. Station abbreviations are defined in Table S1

transport model (Hourdin et al., 2013) with variable winds for 1980–2012. This simulation is the T1 (see Section 2 and Table S4), from which the modeled CO₂ concentration field was sampled at each station and analyzed changes in amplitude, as for the observed time series.

Most T1 simulations (except with the ISAM and JULES ecosystem models) produce a significant increase in AMP_{P-T} at boreal (north of 50°N) stations (Figure 1a), though there are differences among models. In comparison with the observed average trend (0.094 ± 0.033 ppm/year) of AMP_{P-T} at the eight boreal stations with a significant increase in AMP_{P-T}, three models show a larger AMP_{P-T} positive trend (CLM4.5: 0.105 ± 0.046 ppm/year; LPJ: 0.101 ± 0.053 ppm/year; VISIT: 0.101 ± 0.059 ppm/year). The T1 simulations also correctly reproduced the absence of a trend for the three boreal stations with no significant trend in observed AMP_{P-T} (BAL, MHD and SHM in Figure 1a), except for ORCHIDEE for MHD and VISIT for SHM.

Similar to trends in AMP_{P-T}, statistically significant increasing AMP_{T-P} is found in the T1 simulation results (except again for ISAM and JULES), consistent with the observed trends. The simulations with ISAM and JULES produce more significant increasing trends in AMP_{T-P} for temperate than boreal and Arctic stations.

Overall, unlike previous studies that have shown a systematic underestimation of AMP trend by ecosystem models, namely the CMIP5 models (Taylor, Stouffer, & Meehl, 2012) and the MsTMIP models (Huntzinger et al., 2013; Wei et al., 2014) at high northern latitudes (Graven et al., 2013; Thomas et al., 2016), we found both underestimation and overestimation of AMP trends from the

TRENDYv2 models (Fig. S4). This phenomenon may be due to different climate forcing (between CMIP5 and other ensembles), partly different terrestrial ecosystem models, and the simulation of transport using different models (LMDZ4 here instead of TM3 and ACTM in Graven et al. (2013) and TM3 in Thomas et al. (2016)).

5 | EFFECTS OF VARIOUS FACTORS ON THE TRENDS IN AMP_{P-T}

To separate the contribution of different driving factors on the trend of AMP_{P-T}, we performed transport simulations with changes in NBP caused by different factors from factorial runs of the TRENDYv2 models, respectively with variable CO₂ only (eCO₂), variable CO₂ and climate, and variable CO₂, climate and land-cover change (Table S4, see Section 2). We further differentiated between the contribution of trends in atmospheric transport from the trends in AMP, using the LMDZ4 transport model with variable transport fields (Dee et al., 2011) but constant NBP, air-sea CO₂ flux and fossil fuel and cement emissions for 1979, so that the trends in AMP from this simulation could be attributed to transport trends only.

The impact of climate change on NBP affecting the AMP_{P-T} trends estimated from the multi-model ensemble mean (MMEM) varies among stations (Figure 2a). We find a positive trend of AMP induced by climate change at boreal atmospheric stations (eight of 11 stations north of 50°N (Figure 2a and Fig. S5b). On average, climate change caused an enhancement of 0.015 ± 0.025 ppm/year in AMP_{P-T} over boreal region (north of 50°N; Figure 3a), which is about

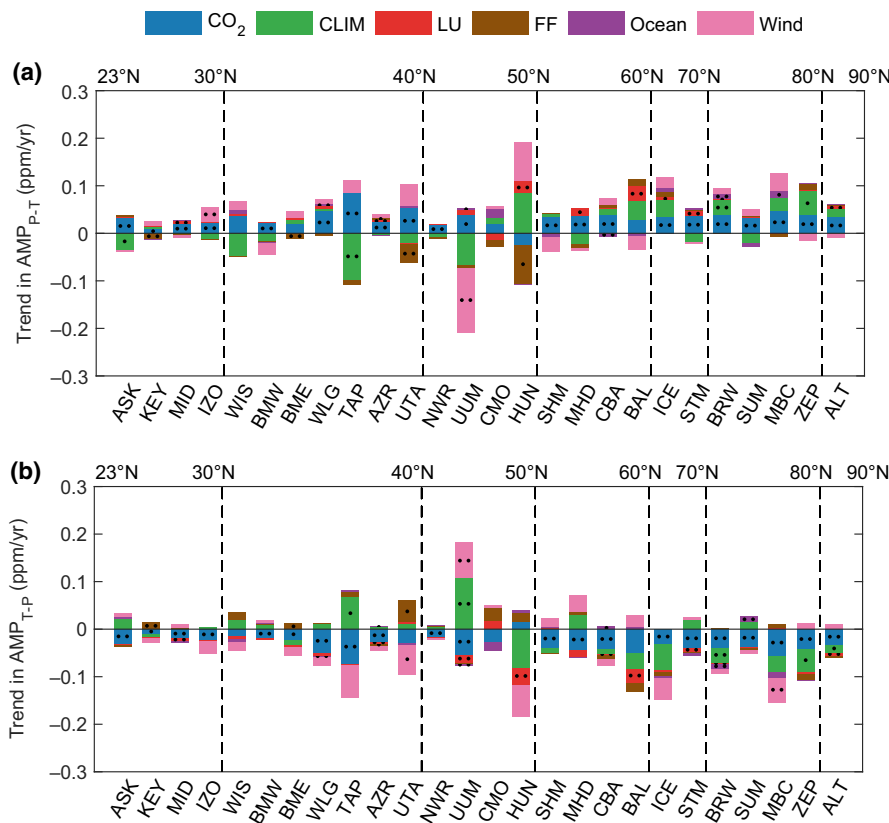


FIGURE 2 Trends in CO₂ seasonal peak-to-trough amplitude (AMP_{P-T}) (a) and trough-to-peak amplitude (AMP_{T-P}) (b) estimated by multi-model ensemble mean (MMEM) under various scenarios for the 26 northern temperate (23–50°N) and boreal (north of 50°N) stations. The results are presented based on the latitudes of the stations. The individual effects of changes in atmospheric CO₂ (“CO₂”), climate (“CLIM”), land use (“LU”), fossil fuel (“FF”), ocean-air carbon flux (“Ocean”), and wind (“Wind”) on the CO₂ seasonal amplitudes were derived from transport simulations (T2–T6), (T3–T2), (T4–T3), (T7–T6), (T8–T6), and T6, respectively (see Section 2 and Table S4). Significant ($p < .05$) trends for each scenario are denoted by two dots, and marginally significant ($p < .10$) trends are denoted by one dot, in the middle of the bars

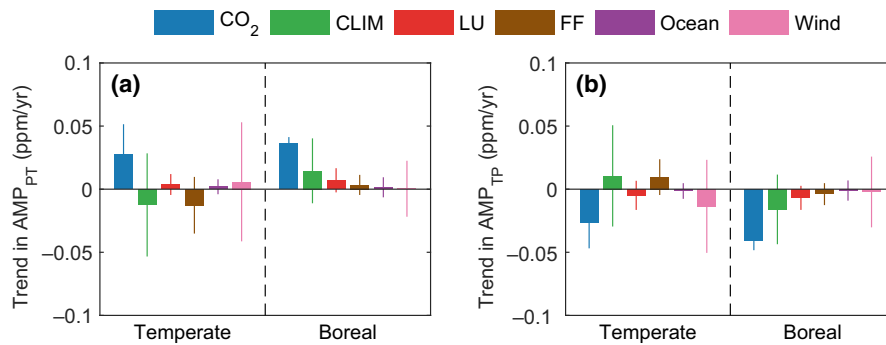


FIGURE 3 Trends in CO₂ seasonal peak-to-trough amplitude (AMP_{p-T}) (a) and trough-to-peak amplitude (AMP_{t-P}) (b) estimated by multi-model ensemble mean (MEM) under different scenarios, averaged over the stations from the northern temperate (23–50°N) and boreal (north of 50°N) region. Model scenario simulations include changes in atmospheric CO₂ (“CO₂”), climate (“CLIM”), land use (“LU”), fossil fuel (“FF”), ocean-air carbon flux (“Ocean”), and wind (“Wind”). Uncertainties are shown by error bars based on the standard deviation of AMP trends across the stations in each region

20% of the observed AMP_{p-T} trend. To have an idea of the potential impact of different climatic factors, we present an analysis on the trends of temperature and precipitation during 1980–2012 in northern hemisphere. As shown in Fig. S5, most northern high-latitude regions show non-significant trends of precipitation. By contrast, a positive trend of temperature was widely found in eastern Siberia and Alaska (Fig. S5), which is also the main footprint area of Barrow station (Piao et al., 2017). This result indicates that temperature is the possible dominant factor on AMP trends at high latitudes, although such positive effects may saturate (Fu et al., 2015; Piao et al., 2014). As shown in Fig. S6a, for the BRW station (71°N), the effect of climate change on AMP_{p-T} is positive mainly during May and June.

In contrast, at the temperate stations (in the band of 23–50°N), the effect of climate change on the AMP_{p-T} trends is mainly negative (10 of the 15 stations), although the impact is not significant (except for TAP at $p < .05$ and ASK marginally significant at $p < .1$). Climate change is modeled to cause an average decrease in AMP_{p-T} of -0.012 ± 0.040 ppm/year at stations in the temperate region (Figure 3a). Analysis of NBP impacted by climate change (Trendy models S2–S1 simulations) shows that climate change alone caused a decrease in CO₂ uptake from April to August in western and central US, eastern Europe, northeast China and Mongolia (Fig. S7b), associated with declining soil moisture driven by rising temperature and decreasing precipitation in these regions (Sitch et al., 2015).

In the simulations of CO₂ with MEM, eCO₂ causes a significant increase in AMP_{p-T} at 10 of the 11 boreal stations (Figure 2a), and the magnitude of trend in AMP_{p-T} driven by eCO₂ (0.036 ± 0.005 ppm/year) is about twice as large as that caused by climate change (Figure 3a). This larger effect of eCO₂ than climate change on the AMP_{p-T} trends in the boreal zone is also present in the simulations with NBP in the individual ecosystem models (Fig. S8a,b). This result does not support previous findings by Forkel et al. (2016), in which the signal of climate change is considered larger than eCO₂ in the observed increase of AMP_{p-T} at high latitudes. We agree, however, that climate change rather than eCO₂ causes the latitudinal difference of trend in AMP_{p-T}. The magnitude of

eCO₂ effect to increase the trend of AMP in temperate regions (0.028 ± 0.023 ppm/year) is comparable to that in boreal regions (Figure 3a), although the effect is significant at fewer stations (nine of 15; Figure 2a). It should be noted that four TRENDY models (CLM4.5, ISAM, LPX and OCN) considered carbon-nitrogen interactions and nitrogen deposition, thus the eCO₂ signal derived from these models also includes the interactive effect of nitrogen deposition. Another simulation with nitrogen deposition using the CLM4 model (Mao et al., 2013; Oleson et al., 2010; see Section 2), however, predicts that the effect of nitrogen deposition on the AMP_{p-T} trend is not significant ($p < .05$) at any of the stations (Fig. S9a), but this result depends on individual model parameterizations (Galloway et al., 2008). Further studies based on multiple models with carbon-nitrogen interactions are thus needed.

Both forest inventory data and model simulation have indicated that afforestation and forest regrowth after the abandonment of agriculture in northern ecosystems have an important role in regional and global carbon balances (FAO, 2015; Houghton et al., 2012; Pan et al., 2011). Most TRENDYv2 DGVMs (except ISAM) in our study predict that land-use change would increase net carbon uptake from April to August in Eastern Europe, China, and central and eastern United States (Fig. S7c). Accordingly, a significant ($p < .05$) or marginally significant ($p < .10$) positive effect of land-use change on the trend in AMP_{p-T} is predicted across six boreal stations and three northern temperate stations (Figure 2a and Fig. S5c), although the magnitude of the signal is generally much smaller than the effect of eCO₂ and climate change. Overall, the positive increase in AMP_{p-T} attributed to land-use change is similar between boreal (0.007 ± 0.009 ppm/year) and northern temperate (0.004 ± 0.008 ppm/year) regions (Figure 3a), suggesting that the latitudinal difference in observed AMP_{p-T} increase (0.07 ± 0.05 ppm/year in the boreal zone and 0.01 ± 0.05 ppm/year in temperate zone) has little linkage with land-use change. It should be noted that, however, large uncertainties remain in estimating the effect of land-use change on the AMP_{p-T} trend, primarily because processes of land-use change and management (eg, wood harvest, shifting cultivation and peat fires) are not considered in

some Trendy models (Table S3) and some critical processes (eg, human settlement, erosion/sequestration and woody encroachment) are absent in all models (Houghton et al., 2012).

Over the past thirty years, global CO₂ emissions from fossil fuel consumption have increased from 5.3 Pg C/year in 1980 to 9.7 Pg C/year in 2012 (Boden et al., 2016; Fig. S10a). However, the pattern of change is not spatially uniform in the Northern Hemisphere. Annual fossil fuel CO₂ emissions is increased significantly in the northern temperate region, but decreased in the boreal region (Fig. S10a). This heterogeneity is also found in the period of April to August, during which AMP_{p-T} is calculated for most northern temperate and boreal stations (Fig. S10b). As a result, effect of changes in fossil fuel carbon emissions on the trend in AMP_{p-T} is opposite between temperate and boreal stations, although the trends in AMP_{p-T} caused by the trends in fossil CO₂ emissions were not significant for most stations. A negative effect of fossil fuel emissions on the AMP_{p-T} trend is simulated for the temperate stations (13 of the 15 stations showing a negative trend with three significant stations and one marginally significant station; Figure 2a), and a positive effect is simulated for most boreal stations (eight of the 11 stations). The absolute value of the AMP_{p-T} trend associated with fossil fuel emissions is generally larger at temperate (average of -0.013 ± 0.022 ppm/year) compared to boreal stations (average of 0.003 ± 0.007 ppm/year; Figure 3a).

A recent study (Horton et al., 2015) demonstrated robust trends in sub-seasonal atmospheric circulation patterns over mid-latitude regions during 1979–2013, particularly in summer and autumn. Such changes in large-scale atmospheric circulation may exert an effect on the trend of CO₂ amplitude. The magnitude of AMP_{p-T} trend caused by transport change is comparable or even larger than the effect of climate change and eCO₂ on NBP at some atmospheric stations, particularly in the temperate zone, although the impact of transport trends on the trend in AMP_{p-T} was significant for only two stations (UUM and IZO; Figure 2a). The magnitude of AMP_{p-T} trend caused by wind is remarkable at UUM (Figure 2a), suggesting the potential role of atmospheric transport. This result is consistent with the recent study showing that increasing seasonal fluxes in lower latitudes have a larger impact on the CO₂ amplitude throughout most of the troposphere compared to increasing seasonal fluxes at higher latitudes due to isentropic transport across latitudes (Barnes et al., 2016).

In terms of effects air-sea fluxes on the trend of AMP_{p-T}, a weak contribution to AMP trends was simulated across most of stations except at BRW (0.010 ppm/year, $p < .05$, 10% of the observed trend) and MBC (0.015 ppm/year, $p < .1$, 16% of the observed trend).

The mechanisms driving the trend in AMP_{p-T} are here analyzed with observations at the Arctic station of BRW (71°N), the longest northern high-latitude CO₂ record showing an increase of amplitude of 35% since 50 years, larger than at the Mauna Loa longest record located in the sub-tropics (Barlow et al., 2015; Forkel et al., 2016; Graven et al., 2013; Gray et al., 2014; Zeng et al., 2014). Our transport simulations with MMEM NBP indicate that AMP_{p-T} at the BRW

station significantly increased by about 0.095 ppm/year from 1980 to 2012, comparable to the observed trend of 0.097 ppm/year (Figure 1a). eCO₂ is identified as the largest contributor of increasing AMP_{p-T} with a trend of 0.039 ppm/year (40% of the observed trend, $p < .05$), followed by climate change with a trend of 0.031 ppm/year (32% of the observed trend, $p < .05$; Fig. S8a,b). The effect of ocean flux is of 0.010 ppm/year (10% of observed trend, $p < .05$), and land-use change has marginally significant contributions (0.003 ppm/year and 3% of observed trend, $p < .1$; Fig. S8c,e). The impacts on the AMP_{p-T} trend were not significant for the other factors such as fossil fuel emissions and transport (Fig. S8d,f).

6 | EFFECTS OF VARIOUS FACTORS ON TRENDS IN AMP_{T-P}

We also assessed the effect of various factors on the trend in AMP_{T-P} with the same NBP and transport model simulations (See Section 2). In contrast to the period of net carbon uptake, climate change accelerates carbon release from boreal ecosystems during the non-carbon uptake period. An increasing AMP_{T-P} (a negative trend in AMP_{T-P} indicates a larger release) is simulated at eight of the 11 boreal stations (one station significant at $p < .05$; two stations marginally significant at $p < .1$; Figure 2b). In contrast, a decreasing AMP_{T-P} (shown with positive trend) is produced at 12 of the 15 temperate stations (one station significant at $p < .05$; one station marginally significant at $p < .1$; Figure 2b). Autumnal warming may increase vegetation productivity by delaying vegetation senescence, as well as accelerate ecosystem respiration (Piao et al., 2008; Vesala et al., 2010). The opposite effect of climate change on the trend in AMP_{T-P} in boreal (-0.016 ± 0.027 ppm/year) and temperate (0.011 ± 0.040 ppm/year) regions (Figure 3b) is therefore probably due to their different magnitudes of the response of vegetation productivity (GPP) and ecosystem respiration (TER) to climate change. Indeed, the model show that the climate change induced increase of TER is greater than that of GPP in high northern latitudes, whereas the increase of GPP is larger in temperate regions (Fig. S11).

Simulation of atmospheric CO₂ from MMEM NBP produce an increasing AMP_{T-P} in response to eCO₂ at 25 of the 26 temperate and boreal stations (19 stations significant at $p < .05$, two stations marginally significant at $.05 < p < .1$; Figure 2b). NBP from six out of the eight terrestrial ecosystem models (except ISAM and JULES) also produces an enhancing AMP_{T-P} from eCO₂ (Fig. S12a). This result indicates that an acceleration of carbon release during the period of net carbon release is as an indirect effect of the NBP response to eCO₂. This acceleration is due to the increment in carbon storage caused by the enhancement of net carbon uptake during the period of carbon uptake under the effect of eCO₂, which stimulates ecosystem respiration during the non-carbon uptake period (Fig. S13). Similarly, we also found enlargement of AMP_{T-P} in response to land-use change (significant at nine of the 26 stations, Figure 2b).

Similar to the effect on AMP_{p-T}, the contribution of fossil fuel CO₂ emissions, air-sea fluxes and transport on the trends in AMP_{T-P}

are significant only at a minority of stations (only one, four and two stations at $p < .05$ for the effect of fossil fuel, air-sea fluxes and transport, respectively; Figure 2b). However, the magnitude of signal induced by transport and fossil fuel emissions is generally remarkable over temperate region (Figure 3b), causing an average impacts of -0.014 ± 0.036 ppm/year and 0.010 ± 0.014 ppm/year in the trend of AMP_{P-T} , respectively.

Overall, the observed significant enlargement of AMP_{T-P} at the BRW station (-0.090 ppm/year) is mainly driven by eCO_2 (-0.038 ppm/year and 42% of the observing trend, $p < .05$), climate change (0.032 ppm/year and 35% of the observing trend, $p < .05$), ocean flux change (-0.010 ppm/year and 11% of the observing trend, $p < .05$) and land-use change (-0.003 ppm/year and 4% of the observing trend, $p < .05$).

7 | CONCLUSION

Unlike previous studies based on one model only (Forkel et al., 2016; Zeng et al., 2014), our results based on an ensemble of models to capture the trends in amplitude suggest that rising atmospheric CO_2 concentration is the primary driver of enhancement of both AMP_{P-T} and AMP_{T-P} , although climate change plays a critical role and contributes largely to the latitudinal differences in the AMP trend. In addition, the effects of other factors such as land-use change, fossil fuel emissions, ocean flux, and transport on the trends in AMP_{P-T} and AMP_{T-P} are not statistically significant at most stations, but still large enough to cancel out the effect of eCO_2 at some temperate stations where the observed seasonal CO_2 trends are small. However, the uncertainties in the forcing data on land-use change and fossil fuel emission at the moment do not allow an unequivocal statement on the contribution of these factors, and further studies based on spatially and temporally explicit historical data sets, including land use and fossil fuel emission are needed. Finally, rising atmospheric CO_2 concentration has an opposite implication in the northern ecosystem carbon balance between the period of carbon uptake (trend in AMP_{P-T}) and the period of carbon release (trend in AMP_{T-P}), due to the lagged effects of increases in carbon storage during the period of carbon uptake on the carbon cycle in the period of carbon release. Our results not only provide insights for large-scale field experiments, but also highlight the importance of understanding processes of the carbon release during the non-growing season, which is critical for reliable projections of the global carbon cycle, and thus, the future climate change.

ACKNOWLEDGEMENTS

We thank the TRENDY modelers for contributing the model outputs. This study was supported by the National Natural Science Foundation of China (41530528), the BELSPO STEREO project ECOPROPHET (SR00334), the 111 Project (B14001), and the National Youth Top-notch Talent Support Program in China. Philippe Ciais, Ivan A Janssens and Josep Peñuelas acknowledge support from the

European Research Council through Synergy grant ERC-2013-SyG-610028 "P-IMBALANCE".

ORCID

Shilong Piao  <http://orcid.org/0000-0001-8057-2292>

Tao Wang  <http://orcid.org/0000-0002-1323-8697>

REFERENCES

- Andres, R. J., Gregg, J. S., Losey, L., Marland, G., & Boden, T. A. (2011). Monthly, global emissions of carbon dioxide from fossil fuel consumption. *Tellus*, *63B*, 309–327.
- Aumont, O., Maier-Reimer, E., Blain, S., & Monfray, P. (2003). An ecosystem model of the global ocean including Fe, Si, P colimitations. *Global Biogeochemical Cycles*, *17*, 1060. <https://doi.org/10.1029/2001gb001745>
- Bacastow, R. B., Keeling, C. D., & Whorf, T. P. (1985). Seasonal amplitude increase in atmospheric CO_2 concentration at Mauna Loa, Hawaii, 1959–1982. *Journal of Geophysical Research: Atmospheres*, *90*, 10529–10540.
- Barlow, J. M., Palmer, P. I., Bruhwiler, L. M., & Tans, P. (2015). Analysis of CO_2 mole fraction data: First evidence of large-scale changes in CO_2 uptake at high northern latitudes. *Atmospheric Chemistry and Physics*, *15*, 13739–13758.
- Barnes, E. A., Parazoo, N., Orbe, C., & Denning, A. S. (2016). Isentropic transport and the seasonal cycle amplitude of CO_2 . *Journal of Geophysical Research: Atmospheres*, *121*, 8106–8124. <https://doi.org/10.1002/2016JD025109>
- Boden, T. A., Marland, G., & Andres, R. J. (2016). Global, regional, and national fossil-fuel CO_2 Emissions. Carbon Dioxide Information Analysis Center, Oak Ridge National Laboratory, U.S. Department of Energy, Oak Ridge, TN, U.S.A. https://doi.org/10.3334/cdiac/00001_v2016
- Buitenhuis, E. T., Rivkin, R. B., Sailley, S., & Le Quéré, C. (2010). Biogeochemical fluxes through microzooplankton. *Global Biogeochemical Cycles*, *24*, GB4015. <https://doi.org/10.1029/2009gb003601>
- Cotrim da Cunha, L., Buitenhuis, E. T., Le Quéré, C., Giraud, X., & Ludwig, W. (2007). Potential impact of changes in river nutrient supply on global ocean biogeochemistry. *Global Biogeochemical Cycles*, *21*, GB4007. <https://doi.org/10.1029/2006gb002718>
- Dee, D. P., Uppala, S. M., Simmons, A. J., Berrisford, P., Poli, P., Kobayashi, S., ... Vitart, F. (2011). The ERA-Interim reanalysis: Configuration and performance of the data assimilation system. *Quarterly Journal of the Royal Meteorological Society*, *137*, 553–597.
- Foley, J. A., DeFries, R., Asner, G. P., Barford, C., Bonan, G., Carpenter, S. R., ... Snyder, P. K. (2005). Global consequences of land use. *Science*, *309*, 570–574.
- Food and Agriculture Organization of the United States (FAO) (2015). Global Forest Resources Assessment 2015: How are the world's forests changing? Retrieved from <http://www.fao.org/forest-resources-assessment/en/>
- Forkel, M., Carvalhais, N., Rödenbeck, C., Keeling, R., Heimann, M., Thonicke, K., ... Reichstein, M. (2016). Enhanced seasonal CO_2 exchange caused by amplified plant productivity in northern ecosystems. *Science*, *351*, 696–699.
- Fu, Y. H., Zhao, H., Piao, S., Peaucelle, M., Peng, S., Zhou, G., ... Janssens, I. A. (2015). Declining global warming effects on the phenology of spring leaf unfolding. *Nature*, *526*, 104–107.
- Galloway, J. N., Townsend, A. R., Erisman, J. W., Bekunda, M., Cai, Z., Freney, J. R., ... Sutton, M. A. (2008). Transformation of the nitrogen cycle: Recent trends, questions, and potential solutions. *Science*, *320*, 889–892.
- Graven, H. D., Keeling, R. F., Piper, S. C., Patra, P. K., Stephens, B. B., Wofsy, S. C., ... Bent, J. D. (2013). Enhanced seasonal exchange of CO_2 by northern ecosystems since 1960. *Science*, *341*, 1085–1089.

- Gray, J. M., Frolking, S., Kort, E. A., Ray, D. K., Kucharik, C. J., Ramanakutty, N., & Friedl, M. A. (2014). Direct human influence on atmospheric CO₂ seasonality from increased cropland productivity. *Nature*, 515, 398–401.
- Horton, D. E., Johnson, N. C., Singh, D., Swain, D. L., Rajaratnam, B., & Diffenbaugh, N. S. (2015). Contribution of changes in atmospheric circulation patterns to extreme temperature trends. *Nature*, 522, 465–469.
- Houghton, R. A., House, J. I., Pongratz, J., Van Der Werf, G. R., DeFries, R. S., Hansen, M. C., ... Ramanakutty, N. (2012). Carbon emissions from land use and land-cover change. *Biogeosciences*, 9, 5125–5142.
- Hourdin, F., Foujols, M. A., Codron, F., Guemas, V., Dufresne, J.-L., Bony, S., ... Bopp, L. (2013). Impact of the LMDZ atmospheric grid configuration on the climate and sensitivity of the IPSL-CM5A coupled model. *Climate Dynamics*, 40, 2167–2192.
- Huntzinger, D. N., Schwalm, C., Michalak, A. M., Schaefer, K., King, A. W., Wei, Y., ... Zhu, Q. (2013). The North American carbon program multi-scale synthesis and terrestrial model intercomparison project - Part 1: Overview and experimental design. *Geoscientific Model Development*, 6, 2121–2133.
- Hurt, G. C., Chini, L. P., Frolking, S., Betts, R. A., Feddema, J., Fischer, G., ... Wang, Y. P. (2011). Harmonization of land-use scenarios for the period 1500–2100: 600 years of global gridded annual land-use transitions, wood harvest, and resulting secondary lands. *Climatic change*, 109, 117–161.
- Kalnay, E., Kanamitsu, M., Kistler, R., Collins, W., Deaven, D., Gandin, L., ... Reynolds, R. (1996). The NCEP/NCAR 40-year reanalysis project. *Bulletin of the American Meteorological Society*, 77, 437–471.
- Keeling, C. D., Chin, J. F. S., & Whorf, T. P. (1996). Increased activity of northern vegetation inferred from atmospheric CO₂ measurements. *Nature*, 382, 146–149.
- Keeling, C. D., & Whorf, T. P. (2005). Atmospheric carbon dioxide record from Mauna Loa. Trends: A Compendium of Data on Global Change. Carbon Dioxide Information Analysis Center, Oak Ridge National Laboratory, Oak Ridge, TN.
- Kohlmaier, G. H., Siré, E., Janecek, A., Keeling, C. D., Piper, S. C., & Revelle, R. (1989). Modelling the seasonal contribution of a CO₂ fertilization effect of the terrestrial vegetation to the amplitude increase in atmospheric CO₂ at Mauna Loa Observatory. *Tellus*, 41B, 487–510.
- Lamarque, J. F., Kiehl, J. T., Brasseur, G. P., Butler, T., Cameron-Smith, P., Collins, W. D., ... Thornton, P. (2005). Assessing future nitrogen deposition and carbon cycle feedback using a multimodel approach: Analysis of nitrogen deposition. *Journal of Geophysical Research: Atmospheres*, 110, D19303. <https://doi.org/10.1029/2005JD005825>
- Mao, J., Ribes, A., Yan, B., Shi, X., Thornton, P. E., Séférian, R., ... Lian, X. (2017). Human-induced greening of the northern extratropical land surface. *Nature Climate Change*, 6, 959–963.
- Mao, J., Shi, X., Thornton, P. E., Hoffman, F. M., Zhu, Z., & Myneni, R. B. (2013). Global latitudinal-asymmetric vegetation growth trends and their driving mechanisms: 1982–2009. *Remote Sensing*, 5, 1484–1497.
- Masarie, K. A., Peters, W., Jacobson, A. R., & Tans, P. P. (2014). ObsPack: A framework for the preparation, delivery, and attribution of atmospheric greenhouse gas measurements. *Earth System Science Data*, 6, 375–384.
- Oleson, K. W., Lawrence, D. M., Gordon, B., Flanner, M. G., Kluzek, E., Peter, J., ... Decker, M. (2010). *Technical description of version 4.0 of the Community Land Model (CLM)*. Boulder, CO: NCAR Technical Note NCAR/TN 478+STR; The National Center for Atmospheric Research (NCAR).
- Pan, Y., Birdsey, R. A., Fang, J., Houghton, R., Kauppi, P. E., Kurz, W. A., ... Hayes, D. (2011). A large and persistent carbon sink in the world's forests. *Science*, 333, 988–993.
- Piao, S., Ciais, P., Friedlingstein, P., Peylin, P., Reichstein, M., Luysaert, S., ... Vesala, T. (2008). Net carbon dioxide losses of northern ecosystems in response to autumn warming. *Nature*, 451, 49–52.
- Piao, S., Liu, Z., Wang, T., Peng, S., Ciais, P., Huang, M., ... Tans, P. P. (2017). Weakening temperature control on the interannual variations of spring carbon uptake across northern lands. *Nature Climate Change*, 7, 359–363.
- Piao, S., Nan, H., Huntingford, C., Ciais, P., Friedlingstein, P., Sitch, S., ... Chen, A. (2014). Evidence for a weakening relationship between interannual temperature variability and northern vegetation activity. *Nature Communications*, 5, 5018.
- Randerson, J. T., Thompson, M. V., Conway, T. J., Fung, I. Y., & Field, C. B. (1997). The contribution of terrestrial sources and sinks to trends in the seasonal cycle of atmospheric carbon dioxide. *Global Biogeochemical Cycles*, 11, 535–560.
- Sitch, S., Friedlingstein, P., Gruber, N., Jones, S. D., Murray-Tortarolo, G., Ahlström, A., ... Myneni, R. (2015). Recent trends and drivers of regional sources and sinks of carbon dioxide. *Biogeosciences*, 12, 653–679.
- Taylor, K. E., Stouffer, R. J., & Meehl, G. A. (2012). An overview of CMIP5 and the experiment design. *Bulletin of the American Meteorological Society*, 93, 485–498.
- Thomas, R. T., Prentice, I. C., Graven, H., Ciais, P., Fisher, J. B., Hayes, D. J., ... Zeng, N. (2016). Increased light-use efficiency in northern terrestrial ecosystems indicated by CO₂ and greening observations. *Geophysical Research Letters*, 43, 11339–11349.
- Thoning, K. W., Tans, P. P., & Komhyr, W. D. (1989). Atmospheric carbon dioxide at Mauna Loa observatory. II - Analysis of the NOAA GMCC data, 1974–1985. *Journal of Geophysical Research*, 94, 8549–8565.
- Vesala, T., Launiainen, S., Kolari, P., Pumpanen, J., Sevanto, S., Hari, P., ... Ciais, P. (2010). Autumn temperature and carbon balance of a boreal Scots pine forest in Southern Finland. *Biogeosciences*, 7, 163–176.
- Wei, Y., Liu, S., Huntzinger, D. N., Michalak, A. M., Viovy, N., Post, W. M., ... Shi, X. (2014). The North American carbon program multi-scale synthesis and terrestrial model intercomparison project: Part 2 - Environmental driver data. *Geoscientific Model Development*, 7, 2875–2893.
- Wenzel, S., Cox, P. M., Eyring, V., & Friedlingstein, P. (2016). Projected land photosynthesis constrained by changes in the seasonal cycle of atmospheric CO₂. *Nature*, 538, 499–501.
- Zeng, N., Zhao, F., Collatz, G. J., Kalnay, E., Salawitch, R. J., West, T. O., & Guanter, L. (2014). Agricultural green revolution as a driver of increasing atmospheric CO₂ seasonal amplitude. *Nature*, 515, 394–397.

SUPPORTING INFORMATION

Additional Supporting Information may be found online in the supporting information tab for this article.

How to cite this article: Piao S, Liu Z, Wang Y, et al. On the causes of trends in the seasonal amplitude of atmospheric CO₂. *Glob Change Biol*. 2018;24:608–616. <https://doi.org/10.1111/gcb.13909>